IEEE Photonics Journal
An IEEE Photonics Society Publication

Open Access

Near-Infrared Supercontinuum and Ultrashort Pulses Generated Based on Phase-Mismatched Cascaded Frequency Conversion in DSTMS Crystal

Volume 12, Number 3, June 2020

Junyu Qian
Yingying Ding
Liwei Song
Zhe Liu
Yafeng Bai
Pengfei Wang
Beijie Shao
Yanyan Li
Yujie Peng
Ye Tian
Yuxin Leng
Ruxin Li

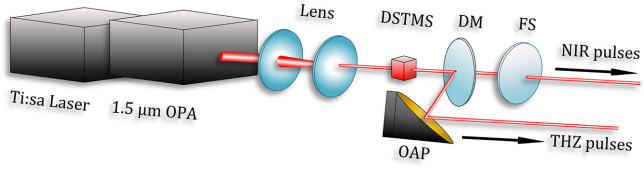

DOI: 10.1109/JPHOT.2020.2992030

Near-Infrared Supercontinuum and Ultrashort Pulses Generated Based on Phase-Mismatched Cascaded Frequency Conversion in DSTMS Crystal

Junyu Qian,[1,2] Yingying Ding,[1,2] Liwei Song,[1] Zhe Liu,[1] Yafeng Bai,[1] Pengfei Wang,[1,2] Beijie Shao,[1,2] Yanyan Li,[1] Yujie Peng,[1,3] Ye Tian,[1,3] Yuxin Leng,[1,3] and Ruxin Li[1,3]

[1]State Key Laboratory of High Field Laser Physics, Shanghai Institute of Optics and Fine Mechanics, Chinese Academy of Sciences, Shanghai 201800, China
[2]Center of Materials Science and Optoelectronics Engineering, University of Chinese Academy of Sciences, Beijing 100049, China
[3]CAS Center for Excellence in Ultra-intense Laser Science, Shanghai 201800, China

DOI:10.1109/JPHOT.2020.2992030

Manuscript received March 30, 2020; revised April 23, 2020; accepted April 29, 2020. Date of publication May 4, 2020; date of current version May 26, 2020. This work was supported in part by the Strategic Priority Research Program of the Chinese Academy of Sciences (XDB1603), in part by the National Natural Science Foundation of China under Grants 11127901, 61925507, 11874372, and 11922412, in part by International S&T Cooperation Program of China (2016YFE0119300), in part by Youth Innovation Promotion Association CAS, 100 Talents Program of CAS, Program of Shanghai Academic/Technology Research Leader (18XD1404200), in part by Shanghai Municipal Science and Technology Major Project (2017SHZDZX02), in part by Shanghai Rising-Star Program (2019-jmrh1-kj1), and in part by Shanghai Pujiang Talents Program (19PJ1410500). Corresponding authors: Liwei Song; Ye Tian; Yuxin Leng (e-mail: slw@siom.ac.cn; tianye@siom.ac.cn; lengyuxin@mail.siom.ac.cn)

Abstract: A near-infrared (NIR) supercontinuum and ultrashort pulses are generated via phase-mismatched cascaded frequency conversion in DSTMS (4-N, N-dimethylamino-4'-N'-methyl-stilbazolium 2, 4, 6-trimethylbenzenesulfonate) crystal. NIR pulses with a central wavelength of 1.5 μm and 63 fs pulse duration are incident into the crystal, and the spectrum is broadened to over 1200–2100 nm. Compensating the dispersion by fused silica, ultrashort NIR pulses with 16.6 fs pulse duration are obtained. Meanwhile, intense single-cycle terahertz pulses are generated via optical rectification in DSTMS crystal.

Index Terms: Ultrafast technology, pulse compression, nonlinearity, terahertz.

1. Introduction

Few-Cycle near-infrared (NIR) laser pulses are currently a hot topic because they are short enough to explore temporal dynamics at the atomic level, such as chemical reactions, electron motion, and so on. Benefit from the broadband spectrum and high peak intensity, few-cycle NIR laser pulses are also widely used in coherently exciting and controlling matter on a microscopic level. Currently, they have been used for various physical researches, such as high harmonic generation (HHG) [1], [2], the photoionization of atomic clusters [3], electron localization in molecular dissociation [4], electron dynamic control [5], and so on. In addition, few-cycle NIR laser pulses are also used in the generation and control of single-cycle pulses in terahertz (THz) spectral region [6], [7].

Over the past two decades, various techniques have been studied to produce intense few-cycle NIR laser pulses. Broadband optical parametric amplification (OPA) and optical parametric chirped-pulse amplification (OPCPA) are able to produce millijoule level few-cycle NIR pulses with 20% energy conversion efficiency by considering a trade-off between the gain bandwidth and the damage threshold of the nonlinear crystals [8]–[12]. Because of the excellent performance and vast potential applications, broadband OPA/OPCPA are referred as the third generation femtosecond technology [13]. While, it is expensive and complicate to construct and operate such a system. Another widely used technology is the combination of spectral broadening in noble gas and dispersion compensation in bulk material [13]–[16]. With this approach, it is convenient to obtain few-cycle NIR pulses based on a commercial OPA device. However, the filament in the gas limits the peak intensity and stability. Cross-polarized wave (XPW) in inorganic nonlinear crystals provides a stable, high contrast and compact few-cycle NIR source [17]. Nevertheless due to the intrinsic properties of the XPW process, the output power is limited to tens of μJ with a conversion efficiency of lower than 15%. Cascaded phase-mismatched second-harmonic generation process has been demonstrated in lithium niobate crystal for NIR spectrum broadening and pulse self-compression [18]. A. Trisorio et al performed this process in an organic DAST (4-N, N-dimethylamino-4'-N'-methylstilbazolium tosylate) crystal and generated octave-spanning, 12.5 fs NIR pulses [19]. In their work, the pump pulse was pre-compressed to 18 fs through filamentation which also restricted the efficiency and stability. Recently, phase-mismatched cascading frequency conversion in other bulk materials has also been applied for laser pulse compression [20], [21].

In this letter, we experimentally demonstrate the generation of NIR supercontinuum and few-cycle pulses using phase-mismatched cascaded frequency conversion in an organic crystal DSTMS (4-N, N-dimethylamino-4'-N'-methyl-stilbazolium 2, 4, 6-trimethylbenzenesulfonate). Cascaded frequency conversion is a kind of self-defocusing Kerr-like effect. It can be achieved with cascaded harmonic generation. When the crystal angle is rotated to maximize the effective nonlinear coefficient, the frequency conversion process lacks phase matching ($\triangle k \neq 0$), so that the pump pulses will experience a self-defocusing Kerr-like process. Since this technique does not need to meet the phase matching condition, it can use the large effective nonlinear coefficient of the crystal over the entire propagation length. Meanwhile, it is a self-defocusing Kerr-like nonlinearity, which means it allows the technique to be up-scalable to millijoule energy by using a large aperture crystal. DSTMS is an organic ionic crystal with a chemical composition. It has good transmittance in the NIR region. And due to its high second-order susceptibility $d_{111} = 214 \pm 20$ pm/V [18], which is almost an order of magnitude higher than the one of the dielectric or semiconductor crystals previously studied in the literature, it is well suited for cascaded frequency conversion. Moreover, DSTMS is a promising crystal for the generation of high field single-cycle THz pulses via optical rectification [22]–[24]. Therefore, the DSTMS crystal is an effective and promising material for generating both few-cycle NIR pulses and intense THz pulses. In the present work, we use the cascading frequency conversion effect of DSTMS crystal to generate a supercontinuum spectrum over 1200–2100 nm, and compensate the dispersion by fused silica (FS) plates. Thereby 16.6 fs (nearly 3 optical cycles) few-cycle NIR pulses was obtained. The output energy is 31 μJ with a transmission efficiency of 35%. Meanwhile, single-cycle THz pulses with a peak field of 220 kV/cm are generated from the same device.

2. Experimental Setup and Results

The schematic of NIR few-cycle pulses generation based on phase-mismatched cascaded frequency conversion in DSTMS crystal is presented in Fig. 1(a). The setup consists of a Ti:sapphire femtosecond laser (Astrella, Coherent Inc.), a home-made two-stage OPA device [25], a beam down-collimator, a 5 mm $\times$ 5 mm $\times$ 0.6 mm DSTMS crystal and FS plates. The OPA device driven by a Ti:sapphire laser delivers NIR pulses with 63 fs pulse duration and 1.5 μm central wavelength. After the beam down-collimator, pulses with 88 μJ pulse energy and 1.5 mm diameter are incident into the DSTMS crystal, which corresponding to an input intensity of $\sim$80 GW/cm^2.

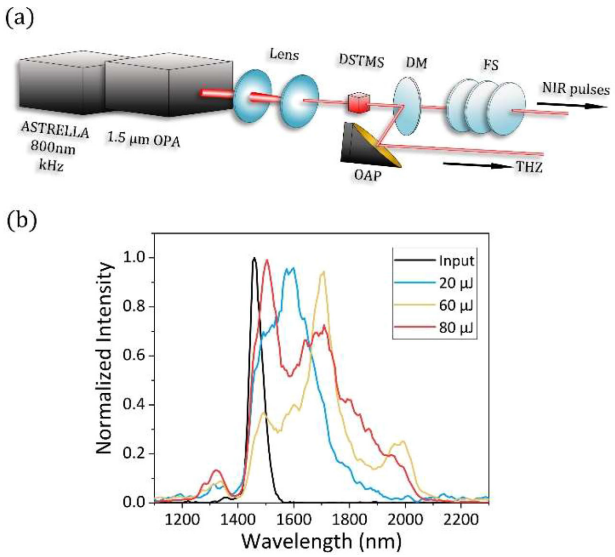

Fig. 1. (a) The experimental setup. (b) The spectra after the DSTMS crystal for different input energy.

The supercontinuum generation using DSTMS crystal is based on phase-mismatched cascaded frequency conversion. During this process, due to the $\chi^2(2\omega;\omega;\omega)$ nonlinearity, the fundamental wave (FW, ω_1) is converted into the second harmonic (SH, $\omega_2 = 2\omega_1$) in a coherence length $\pi/\Delta k$. While because of the absence of phase matching, there is only weak SH conversion occurring. And then after another coherence length, the SH is converted back to the FW via $\chi^2(2\omega;2\omega;-\omega)$ nonlinearity. During the propagation in the DSTMS crystal, this cascade process is repeated and the FW experiences a Kerr-like nonlinear effect. The Kerr-like nonlinear refractive index is proportional to the intensity, $\Delta n = n_{casc} I$. In strong phase mismatched process, $n_{casc} \approx -2\omega_1 d_{eff}^2/c^2\varepsilon_0 n_1^2 n_2 \Delta k$ [26], where $\Delta k = k_2 - 2k_1 = \frac{n_2\omega_2}{c} - 2\frac{n_1\omega_1}{c}$ (k_1 and k_2 are the wave vectors of the fundamental and second-harmonic waves). However, the refractive index change caused by the Kerr effect n_{Kerr} also exists in the crystal simultaneously, therefore if the cascade nonlinearity plays a major role, $|n_{casc}| > n_{Kerr}$ must be satisfied.

Accompanying with the cascaded frequency conversion, an effective negative Kerr-like nonlinearity is generated. While the DSTMS crystal has a positive dispersion, which is helpful to realize pulse self-compression [22]. As a consequence, the pulse has already been self-compressed at the exit of the crystal. However, there is still positive dispersion left, and the FS (negative dispersion at 1500 nm) plates can be employed to compensate for the residual dispersion.

Fig. 1(b) shows the spectra after the DSTMS crystal for different input energy measured by a near-infrared spectrometer (NIR Quest 512, Ocean Optics Inc.). As the input energy increases, the spectral range expands gradually. When the input energy is 80 μJ, the spectrum is broadened to 2100 nm in the long wavelength direction, while in the short wavelength direction, the spectrum is only broadened to 1200 nm and the intensity is relatively weak. The main reason is that the absorption coefficient of DSTMS crystal is much higher at the wavelength below 700 nm [22], thus the SH of short wavelength is strongly absorbed in the crystal, so that only the SH of long wavelength components can be back-converted into the FW.

The NIR pulse energy after DSTMS is 43 μJ, corresponding to a transmittance of 49%. After dispersion compensation, the measured pulse energy is 31 μJ. However, limited by the input pulse energy, the maximum output pulse energy of this DSTMS crystal is not achieved in the experiment. Meanwhile, because of the losses induced by the DSTMS crystal and the uncoated FS plates, the overall transmission efficiency is lower than expected. The loss can be significantly reduced by using anti-reflection coated FS plates. According to the size of the crystal we use, an output pulse energy in the order of hundreds of microjoules can be supported.

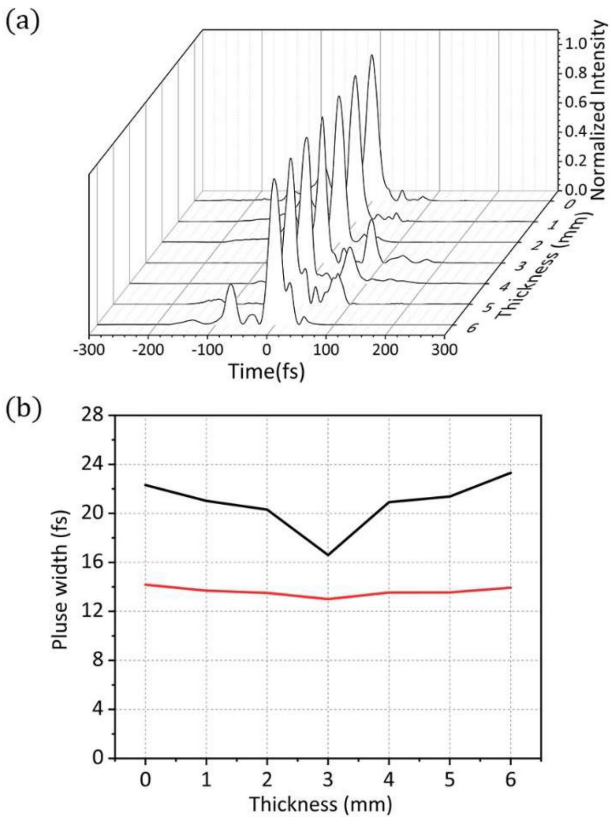

Fig. 2. (a) Evolution of temporal shapes with fused silica thicknesses. (b) The pulse widths (black line) and Fourier transform limit pulse widths (red line) with fused silica thicknesses.

We measured the evolution of pulse width with different FS thicknesses by a home-made second-harmonic-generation frequency-resolved optical gating (SHG-FROG) setup [27]. The results are shown in Fig. 2. Without the FS plates, the pulse width directly emitted from the DSTMS crystal is 22.3 fs. By inserting the FS plates after the DSTMS crystal, the temporal shape changes with the thickness as shown in Fig. 2(a). Fig. 2(b) shows the changes in pulse width and the corresponding Fourier transform limit (FTL) pulse width calculated from the retrieved spectrum.

After adjusting the thickness of the FS plates, it is found that the optimal thickness is 3 mm, the temporal and spectral characterizations of the compressed pulse retrieved from the SHG-FROG device are shown in Fig. 3. It indicates the pulse duration of 16.6 fs is achieved, corresponding to 2.9 optical cycles and 1.28 FTL (FTL = 13.0 fs) at 1700 nm. The error of the FROG inversion is about 1.3%. And it can be seen from Fig. 3(c) that there are satellite pulse accompanying the main pulse. This is a signature of the residual third-order dispersion which cannot be compensated for by the simple bulk compression scheme applied in our experiment. Fig. 3(d) shows the reconstructed spectrum (blue) and phase (red), which is close to the actual spectrum measured by the spectrometer.

Accompanying with the NIR spectral broadening, high field THz pulses are generated via optical rectification in DSTMS. Characterized by electro-optic sampling (EOS) with a 100-μm thick GaP crystal [28], the THz electric field and spectrum are shown in Fig. 4. And the peak field is 220kV/cm, calculated from the EOS signal [29].

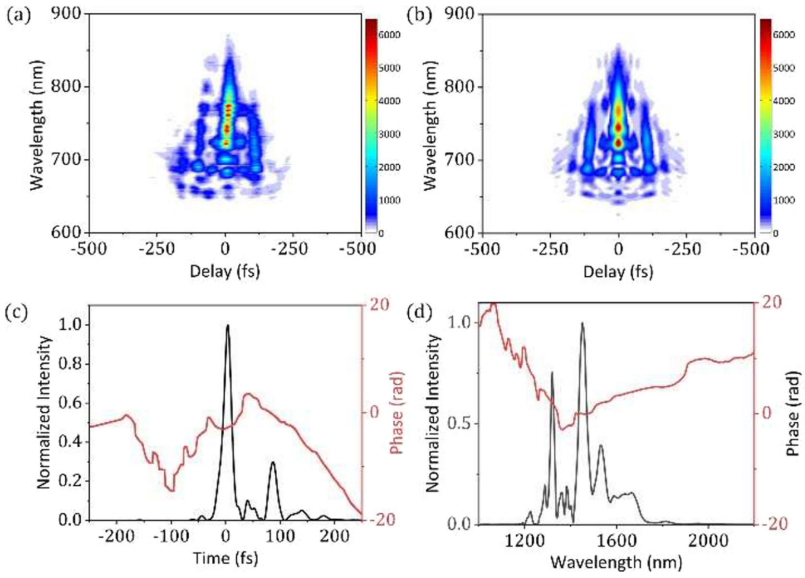

Fig. 3. Temporal characterization of the compressed pulse. (a) Measured and (b) retrieved SHG-FROG traces. (c) Reconstructed pulse envelope (blue), which is 16.6 fs (FWHM) and its phase (red). (d) Reconstructed spectrum (blue) and phase (red).

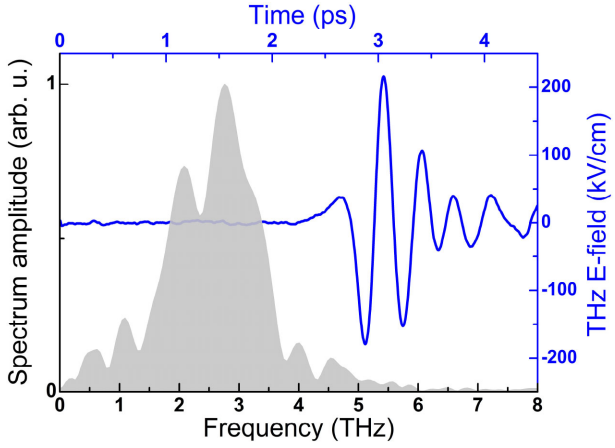

Fig. 4. THz electric field (blue curve) and spectrum (gray shading).

3. Conclusions

In conclusion, we have presented a compact scheme for the generation of few-cycle NIR pulses and high field THz pulses. NIR pulses from a two-stage OPA are spectrally broadened to over 1.2–2.1 μm by phase-mismatched cascaded frequency conversion in a DSTMS crystal. Compensating the dispersion by 3 mm FS plates, pulses with 16.6 fs pulse duration (2.9 optical cycle) and 31 μJ pulse energy are achieved. Meanwhile, single-cycle THz pulses with 220 kV/cm peak field are generated via optical rectification in the DSTMS crystal. Using higher input energy and larger crystal, millijoule level few-cycle NIR pulses and tens of MV/cm THz field should be available. The device provides a platform for ultrafast pump-probe experiments in NIR and THz region.

References

[1] T. Popmintchev *et al.*, "Bright coherent ultrahigh harmonics in the keV x-ray regime from mid-infrared femtosecond lasers," *Science*, vol. 336, pp. 1287–1291, 2012.

[2] N. Ishii, K. Kaneshima, K. Kitano, T. Kanai, S. Watanabe, and J. Itatani, "Carrier-envelope phase-dependent high harmonic generation in the water window using few-cycle infrared pulses," *Nat. Commun.*, vol. 5, pp. 1–6, 2014.

[3] S. R. Krishnan *et al.*, "Photoionization of clusters in intense few-cycle near infrared femtosecond pulses," *Phys. Chem. Chem. Phys.*, vol. 16, pp. 8721–8730, 2014.

[4] K. Liu, Q. Zhang, and P. Lu, "Enhancing electron localization in molecular dissociation by two-color mid- and near-infrared laser fields," *Phys. Rev. A*, vol. 86, 2012, Art. no. 033410.

[5] W. Hong, Q. Zhang, Z. Yang, and P. Lu, "Electron dynamic control for the quantum path in the midinfrared regime using a weak near-infrared pulse," *Phys. Rev., A*, vol. 80, 2009, Art. no. 053407.

[6] Y. Bai *et al.*, "Waveform-controlled terahertz radiation from the air filament produced by few-cycle laser pulses," *Phys. Rev. Lett.*, vol. 108, 2012, Art. no. 255004.

[7] L. Song *et al.*, "Polarization control of terahertz waves generated by circularly polarized few-cycle laser pulses," *Appl. Phys. Lett.*, vol. 103, 2013, Art. no. 261106.

[8] Y. Deng *et al.*, "Carrier-envelope-phase-stable, 12 mJ, 15 cycle laser pulses at 21 μm," *Opt. Lett.*, vol. 37, pp. 4973–4975, 2012.

[9] N. Ishii, K. Kaneshima, K. Kitano, T. Kanai, S. Watanabe, and J. Itatani, "Sub-two-cycle, carrier-envelope phase-stable, intense optical pulses at 16 μm from a BiB_3O_6 optical parametric chirped-pulse amplifier," *Opt. Lett.*, vol. 37, pp. 4182–4184, 2012.

[10] C. Vozzi *et al.*, "High-energy, few-optical-cycle pulses at 1.5 microm with passive carrier-envelope phase stabilization," *Opt. Express*, vol. 14, pp. 10109–10116, 2006.

[11] Y. Yin *et al.*, "High-efficiency optical parametric chirped-pulse amplifier in BiB_3O_6 for generation of 3 mJ, two-cycle, carrier-envelope-phase-stable pulses at 1.7 μm," *Opt. Lett.*,vol. 41, pp. 1142–1145, 2016.

[12] K. H. Hong *et al.*, "High-energy, phase-stable, ultrabroadband kHz OPCPA at 21 μm pumped by a picosecond cryogenic Yb:YAG laser," *Opt. Express*, vol. 19, pp. 15538–15548, 2011.

[13] H. Fattahi *et al.*, "Third-generation femtosecond technology," *Optica*, vol. 1, pp. 45–63, 2014.

[14] B. E. Schmidt *et al.*, "CEP stable 1.6 cycle laser pulses at 1.8 μm," *Opt. Express*, vol. 19, pp. 6858–6864, 2011.

[15] C. Li *et al.*, "Generation of carrier-envelope phase stabilized intense 1.5 cycle pulses at 1.75 μm," *Opt. Express*, vol. 19, pp. 6783–6789, 2011.

[16] F. Theberge, N. Akozbek, W. Liu, A. Becker, and S. L. Chin, "Tunable ultrashort laser pulses generated through filamentation in gases," *Phys. Rev. Lett.*, vol. 97, 2006, Art. no. 023904.

[17] A. Ricci *et al.*, "Generation of high-fidelity few-cycle pulses at 2.1 μm via cross-polarized wave generation," *Opt. Express*, 21, pp. 9711–9721, 2013.

[18] B. B. Zhou, A. Chong, F. W. Wise, and M. Bache, "Ultrafast and octave-spanning optical nonlinearities from strongly phase-mismatched quadratic interactions," *Phys. Rev. Lett.*, 109, 2012, Art. no. 043902.

[19] A. Trisorio, M. Divall, B. Monoszlai, C. Vicario, and C. P. Hauri, "Intense sub-two-cycle infrared pulse generation via phase-mismatched cascaded nonlinear interaction in DAST crystal," *Opt. Lett.*, vol. 39, pp. 2660–2663, 2014.

[20] B. Zhou and M. Bache, "Invited Article: Multiple-octave spanning high-energy mid-IR supercontinuum generation in bulk quadratic nonlinear crystals," *APL Photon.*, vol. 1, 2016, Art. no. 050802.

[21] M. Serdel, J. Brons, G. Arisholm, K. Fritsch, V. Pervak, and O. Pronin, "Efficient high-power untrashort pulse compression in self-defocusing bulk media," *Sci. Rep.*, vol. 7, 2017, Art. no. 1410.

[22] L. Mutter, F. D. J. Brunner, Z. Yang, M. Jazbinsek, and P. Gunter, "Linear and nonlinear optical properties of the organic crystal DSTMS," *J. Opt. Soc. Amer. B*, vol. 24, pp. 2556–2561, 2007.

[23] C. Vicario, A. V. Ovchinnikov, S. I. Ashitkov, M. B. Agranat, V. E. Fortov, and C. P. Hauri, "Generation of 0.9-mJ THz pulses in DSTMS pumped by a $Cr:Mg_2SiO_4$ laser," *Opt. Lett.*, vol. 39, pp. 6632–6635, 2014.

[24] C. Vicario, B. Monoszlai, and C. P. Hauri, "GV/m single-cycle terahertz fields from a laser-driven large-size partitioned organic crystal," *Phys. Rev. Lett.*, vol. 112, 2014, Art. no. 213901.

[25] P. Wang *et al.*, "High-repetition-rate, high-peak-power 1450 nm laser source based on optical parametric chirped pulse amplification," *High Power Laser Sci. Eng.*, vol. 7, 2019, Art. no. E32.

[26] X. Liu, L. Qian, and F. Wise, "High-energy pulse compression by use of negative phase shifts produced by the cascade $\chi^{(2)}:\chi^{(2)}$ nonlinearity," *Opt. Lett.*, vol. 24, pp. 1777–1779, 1999.

[27] Y. Li *et al.*, "Accurate characterization of mid-infrared ultrashort pulse based on second-harmonic-generation frequency-resolved optical gating," *Opt. Laser Technol.*, vol. 120, 2019, Art. no. 105671.

[28] Q. Wu and X. C. Zhang, "Free-space electro-optic sampling of terahertz beams," *Appl. Phys. Lett.*, vol. 67, pp. 3523–3525, 1995.

[29] C. Vicario, C. Ruchert, F. Ardana, and C. Hauri, "Laser-driven generation of intense single-cycle THz field," *Proc. SPIE*, vol. 8261, 2012, Art. no. 82610Z.